



# Microalgae Growth in a Biocathode-Photosynthesis Microbial Desalination Cell: Molecular Characterization, Modeling Study, and Performance Evaluation

Ahmed M. Sadeq<sup>a</sup>, Zainab Z. Ismail<sup>a,\*</sup>

<sup>a</sup> Department of Environmental Engineering, College of Engineering, University of Baghdad, Baghdad, Iraq

## Abstract

This study aimed to comprehensively characterize and identify microalgae inhabiting the biocathode compartment of a photosynthetic microbial desalination cell (PMDC). Also, modeling of microalgae growth in the biocathode was considered as well as the interrelation between the growth of microalgae and dissolved oxygen (DO) generation within the biocathode. The general performance of the PMDC was evaluated based on; (1) organic content removal from the real domestic wastewater fed to the anode compartment, (2) salinity removal from actual seawater in the desalination compartment, and (3) power generation in the PMDC. The results unveiled the presence of two distinct microalgae species, specifically *Coelastrella sp.* and *Mariniradius saccharolyticus*, which were thoroughly characterized using 16S rRNA and ITS gene sequencing within the cathodic chamber of the PMDC. Following sequence editing and trimming, the resulting sequences were meticulously submitted to the NCBI GenBank and juxtaposed with other sequences utilizing the GenBank online BLAST software. Importantly, the obtained data demonstrated a good correlation with coefficients of determination ( $R^2$ ) reaching 0.83, as per the employed kinetic models. Complete removal of up to 99.11% of organic content from the real domestic wastewater was obtained in the PMDC system with maximum efficiency of desalination elimination of 80.95% associated with a maximum power output of 420 mW/m<sup>3</sup> in the system.

**Keywords:** Microbial characterization; microalgae; NCBI GenBank; growth kinetic model; biocathode; photosynthesis microbial fuel cell.

Received on 06/11/2023, Received in Revised Form on 30/12/2023, Accepted on 30/12/2023, Published on 30/03/2024

<https://doi.org/10.31699/IJCPE.2024.1.1>

## 1- Introduction

The direct conversion of waste into high-value energy, clean power, or chemical products is known to be a favorable option for eliminating energy problems and excess sludge in conventional wastewater treatment systems [1]. Microbial fuel cells are biological systems that convert chemical energy in the form of organic substrate in wastewater into electrical energy or other high-value products. This technology offers the possibility to treat wastewater with soluble organic pollutants and generate electric power at the same time [2]. Microbial desalination cells (MDCs) involve 3 separate sections which are; anodic, desalination, and cathodic compartments. The anode is responsible for electron generation. Those electrons travel from the anode electrode to the cathode electrode via an external circuit. The free electrons transfer to the electron acceptors in the cathode compartment in order to complete the electrochemical reactions by carrying out the reduction reaction [3]. In the cathode compartment, electron acceptors help reduce electrons [4]. If instead photosynthetic organisms such as algae are incorporated into the cathode, dissolved oxygen as electron acceptor will be obtained from photosynthesis to facilitate the reduction of electrons at the cathode [5]. The adoption of

biocathodes as catalysts in microbial desalination cells (MDCs) is increasing due to their ability to regenerate and their environmentally friendly nature [6]. The primary goal of employing living organisms for catalysis is to reduce operational expenses, eliminate the need for chemicals and costly metal catalysts, and enable sustainable operations while facilitating the reduction of an oxidizing agent, either directly or indirectly, by accepting electrons from the cathode. Additionally, using biocathodes offers several advantages compared to non-biological cathodes. Various biocatalysts utilized in MDC biocathodes encompass photosynthetic bacteria [7], white-rot fungus [8], and algae [6]. Various microbial consortia like nitrifying and denitrifying bacteria and microalgae can be utilized in biocathodes to produce the electron acceptors required for the reaction of reduction at the cathode. Microbial communities, particularly in activated sludge, exhibit significant diversity, making their comprehensive understanding a challenge. Traditional identification methods, such as microscopy and culture-based techniques, have limitations in distinguishing between unrelated microorganisms and identifying non-culturable species [9]. The advent of molecular biology tools, including Polymerase Chain Reaction (PCR) and DNA oligonucleotide hybridization,



\*Corresponding Author: Email: [dr.zainab.zead@coeng.uobaghdad.edu.iq](mailto:dr.zainab.zead@coeng.uobaghdad.edu.iq)

© 2024 The Author(s). Published by College of Engineering, University of Baghdad.

This is an Open Access article licensed under a [Creative Commons Attribution 4.0 International License](https://creativecommons.org/licenses/by/4.0/). This permits users to copy, redistribute, remix, transmit and adapt the work provided the original work and source is appropriately cited.

has revolutionized microbial ecology, enabling direct genetic analysis of individual microbes and entire communities. In spite of their advantages, there are few studies of molecular characterization of microalgae [9-13]. Moreover, mathematical models of growth kinetics are indispensable for understanding the growth patterns of microalgae and optimizing cultivation conditions. Various process parameters, including light, temperature, nutrients, available carbon, oxygen levels, salinity, and pH, influence the growth rate of microalgal cells.

In this study, molecular characterization of the primary microalgae species utilized in photosynthesis microbial desalination cells (PMDC) was applied. The analysis of the 16S rRNA for blue-green algae and 18S ribosomal RNA (rRNA) for green algae as molecular markers to investigate their genetic composition was employed. Additionally, a mathematical model was adopted to predict and analyze the growth patterns of the microalgal species.

©

## 2- Materials and Methods

### 2.1. Microalgae in the biocathode of PMDC

Microalgae samples were grabbed from Heet city, (Iraq). Before introducing the microalgae into the PMDC system, the grabbed microalgae samples were maintained in an incubator with continuous fluorescent lighting of 4500 lux for 2.5 h in the dark and continuous air circulation. The microalgae were fed with 5 mL of BG11 medium every 7 days. The optical density of the microalgal community was measured before it was introduced into the PMDC system. Fig. 1 illustrates the source and location of microalgae collection as well as the enrichment process and growth of the microalgae.



**Fig. 1.** The Enrichment Process and Growth of the Microalgae

Subsequently, the produced microalgae were injected into the biocathode together with the microalgae cultivation medium, which is regarded as the catholyte. In this study, a BG11 medium was employed as the culture medium [14], which consisted of the following components (in grams per liter): 0.26  $\text{Na}_2\text{HPO}_4$ , 0.74

$\text{KH}_2\text{PO}_4$ , 0.01  $\text{CaCl}_2$ , 0.01 Fe-EDTA, 0.05  $\text{MgSO}_4 \cdot 7\text{H}_2\text{O}$ ,  $\text{Na}_2\text{CO}_3$ , and 1 ml trace elements. The microalgae that were used for this study were changed based on the ideal culture conditions, the required carbon source for the microalgae was  $\text{CO}_2$ , which was supplied by a  $\text{CO}_2$  cylinder (purity of 99.99%). The required light for microalgae cultivation was provided by fluorescent lamps reported by Barahoei et al. [15]. The fluorescent lights were utilized to provide the requisite light for the growth of the microalgae.

### 2.2. Microalgae DNA extraction

DNA extraction from microalgae was performed according to the procedure described by ABIO pure TM Total DNA (ABIO pure, USA). Inoculation of cultivated microalgae with cell lysis and protein digestion, 200  $\mu\text{l}$  lysing buffer, and 20  $\mu\text{l}$  proteinase K solution (20 mg/ml). Then, the mixture was incubated at 56  $^\circ\text{C}$  for 30 min the sample was centrifuged at 10000 rpm for 5 min at 4 $^\circ\text{C}$ . After incubation, 200  $\mu\text{l}$  of absolute ethanol was added to the sample and mixed with a pulsing vortex to agitate the sample thoroughly. All mixtures were carefully transferred to the centrifuge tubes, and centrifuged for 1 min at 6000 x g above (> 8000 rpm). A 600 $\mu\text{l}$  of buffer BW was put in a test tube, and then centrifuged at 6000 x g for 1 min (> 8000 rpm), from buffer BW, 600 $\mu\text{l}$  was added to the centrifuge tube, then centrifuged at 6000 x g for 1 min (> 8000 rpm). A 700 $\mu\text{l}$  of buffer TW was applied and centrifuged at 6000 x g for 1 min (> 8000 rpm). The pass-through was removed and the centrifuge tube was re-inserted into the collection tubes. The centrifuge tube was centrifuged at full speed > 13000 x g for 1 min to get rid of any residual wash buffer, then the centrifuge tube was placed in a fresh 1.5 ml tube. Subsequently, a volume of 100 $\mu\text{l}$  of buffer AE was introduced and subjected to incubation at ambient temperature for a duration of 1 minute. Following this, centrifugation was performed at a speed of 5000 revolutions per minute for a period of 5 minutes. The concentration of extracted DNA was determined using the Quantus Fluorometer (Promega, USA) in order to assess the quality of the samples for further applications. A volume of 1  $\mu\text{l}$  of DNA was combined with 199  $\mu\text{l}$  of diluted Quantifluor dye, followed by an incubation period of 5 minutes at ambient temperature [16, 17].

### 2.3. Identification of green microalgae isolates

In this study, a culture medium specifically used for microalgae served as the bio-catholyte. molecular phylogenetic studies of sequence variation for green microalgae were performed on the internal transcribed spacers of nuclear ribosomal DNA (ITS). DNA extraction was performed using ABIO pure TM Total DNA (ABIO pure, USA). Isolated genomic DNA from *Coelastrella* sp. was used as a template for PCR. The amplification of gene ITS was performed using the universal primer: ITS1: 5'-TCCGTAGGTGAACCTGCGG-3' and ITS4: 5'-TCCTCCGCTTATTGATATGC-3' (Macrogen, Korea).

The PCR reaction was carried out by adding the following components: 12.5  $\mu\text{l}$  GoTaq® G2 Master Mix, 3  $\mu\text{l}$  template DNA (genomic DNA), 1  $\mu\text{l}$  each of the upstream and downstream primers, and 7.5  $\mu\text{l}$  nuclease-free water to make up the volume to 25 $\mu\text{l}$ . The experimental procedure consisted of the subsequent stages: an initial denaturation phase at a temperature of 94 °C for a duration of 5 minutes, followed by a consecutive series of 30 cycles, each including denaturation at 94 °C for a period of 30 seconds, annealing at 55 °C for 30 seconds, and extension at 72 °C for 30 seconds. Additionally, a last extension step was performed at a temperature of 72 °C for a duration of 7 minutes [18].

#### 2.4. Identification of blue-green microalgae isolates

PCR amplification and sequencing of the extracted DNA samples were performed by (Macrogen, Korea). Amplification of the gene fragment of 16S rRNA was performed using universal primers from Thermo Fisher Scientific (USA). The universal primers forward primer 27F (AGAGTTGATCMTGGCTCAG) and reverse primer 1492R (TACGGYTACCTTGTTACGACTT) were used [19]. The PCR reaction was performed by adding 12.5  $\mu\text{l}$  GoTaq® G2 Master Mix, 2  $\mu\text{l}$  template DNA (genomic DNA), 1  $\mu\text{l}$  each of the upstream and downstream primers, and 7.5  $\mu\text{l}$  nuclease-free water to complete the volume to 25  $\mu\text{l}$ . The PCR reaction was performed under the following conditions: initial denaturation was at 95 °C for 5 min, followed by 35 amplification cycles at 95 °C for 30 s, primer annealing temperature of 60 °C for 30 s, and extension at 72 °C for 60 s. The last extension was at 72 °C for 10 min [20].

#### 2.5. Green and Blue- green microalgae classification

The PCR products were added directly to the well and 5 $\mu\text{l}$  was added. Electrical power was turned on at 100V/mA for 1h. DNA migrated from the cathode to the positive anode poles. A gel imaging system was used to view the bands stained with ethidium bromide in the gel. PCR products were sent for Sanger sequencing using ABI3730XL, an automated DNA sequencer from Macrogen Corporation - Korea. The 16 S rRNA and ITS genes sequence was compared using the NCBI Blast Similarity Search Tool. Geneious software was used to analyze the multiple alignments of the sequences. After editing and trimming, the analyzed sequence, it was submitted to NCBI GenBank and compared with other GenBank online BLAST software sequences [21].

#### 2.6. Design, construction, and setup of the sequential cuboid compartments – PMDC

A conventionally designed PMDC with three sequential cuboid compartments, as depicted in Fig. 2, was fabricated from Plexiglas material. The system was set up and operated continuously for a duration of 180 days. In the SC-PMDC configuration, the anode and desalination

chambers were supplied with actual wastewater and seawater, respectively.

The anode compartments in the PMDCs received a steady inflow of real household wastewater at a rate of 1.04 ml/min, facilitated by an adjustable peristaltic pump. Concurrently, the desalination chambers in the PMDCs were provided with a synthetic saline solution at a flow rate of 0.5 ml/min, utilizing a peristaltic pump (BT100S, GOLANDER PUMP, USA). Inoculation of mixed biomass and microalgae was carried out in the anode and cathode chambers, respectively.

The transfer of ionic species in the saline water occurred through the cation (CEM) and anion (AEM) exchange membranes, which functioned to isolate the cathode and anode compartments, respectively.

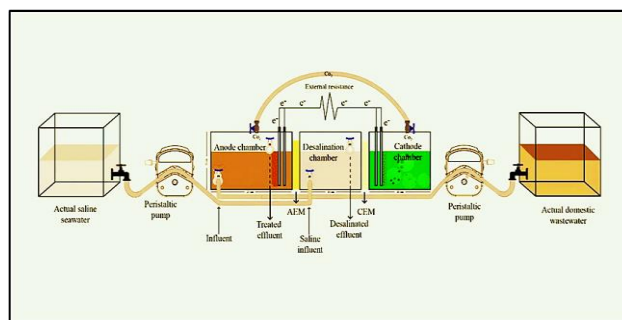


**Fig. 2.** Schematic Diagram of the Sequential Cuboid Compartments PMDC

Dimensions of the SC-PMDC compartments were 25cm x 10cm x 10cm for the bioanode, and 15cm x 10cm x 10cm for the biocathode, whereby, dimensions of the desalination chamber were 15cm x 10cm x 10cm for length, width, and height, respectively. Each of the bioanode and biocathode compartments contained 2 plain graphite electrodes. The effective size of each electrode was 8cm x 2cm x 0.4cm.

#### 2.7. Measurement of microalgae growth

Growth of microalgae was assessed by measurements of the microalgae optical density using a Maxwell® RSC instrument (Promega) at a wavelength of 620 nm. Concentration of dry biomass microalgae was calculated as follows [22]:

$$\text{Microalgae concentration} = \frac{\text{absorbance at wavelength 620 nm}}{0.8702} \quad (1)$$

#### 2.8. Analysis and measurements

Daily measurement of chemical oxygen demand (COD) was performed using the COD analyzer (Model: Lovibond, RD 125, UK). The dissolved oxygen was measured using Dissolved Oxygen meter (Model: waterproof 7031, EZDO, Taiwan), while TDS was measured using TDS meter (Model: portable A1, EZDO, China).

The voltage in the PMDC system was directly measured and recorded by digital multimeters, and then recorded

voltage data were converted to current and power data for further analysis.

### 3- Modelling of Microalgae Growth and Cultivation

In this study, the selected model implicitly considers the prediction of the microalgae growth trends present in the biocathode chamber of the PMDC system.

This model comprises of dynamic equations, a kinetic expression, and a light transfer model. The dynamic equations are founded on two mass balances, assuming a well-mixed photobioreactor. In continuous mode, the change in the number of cells over time is represented by the given expression:

$$\frac{dx}{dt} = \mu X - DX \quad (2)$$

Where;  $\mu$ : is the specific growth rate, (1 per hours). X: cell number of microalgae per unit culture volume (or biomass), (billion cells/L). D: is the dilution rate (1 per hours) [23], i.e, ratio between the flowrate of media and the volume of liquid phase in the bioreactor. This model operates under the assumption that the growth rate of microalgae is constrained by both light intensity and total inorganic carbon levels. The model's growth response was determined by the relationship between these concentrations and their respective optimal values. It employs an exponential decay function, wherein the growth rate rises as the light intensity and total inorganic carbon approach their ideal levels. The following empirical parametric model follows these principles [23]:

$$\mu = \mu_{\max} \left( \frac{E}{K_E + E} \right) \left( \frac{[TIC_{cell}]}{K_{CL} + [TIC_{cell}]} \right) \left( \frac{K_{CI}}{K_{CI} + [TIC_{cell}]} \right) \quad (3)$$

Where;  $\mu_{\max}$ : maximum specific growth rate.  $K_E$ : half saturation constant by light intensity available per cell denoted by E.  $K_{CL}$  and  $K_{CI}$ : the limitation and inhibition constant by  $[TIC_{cell}]$ , respectively.

The total inorganic carbon concentration available per cell is given by the following formula [23]:

$$[TIC_{cell}] = \frac{[TIC]}{X} \quad (4)$$

The intensity of light which is accessible per cell (denoted E) is given by the light transfer model [23]:

$$E = \frac{(I_{in} - I_{out}) \cdot A_r}{V \cdot X} \quad (5)$$

Where;  $I_{in}$ : intensity of incident light,  $I_{out}$ : intensity of outgoing light,  $A_r$ : illuminated area of the bioreactor, V: volume of the liquid phase in the photobioreactor.

The intensity of the outgoing light can be assessed with an analytical expression from the values of the cell number and the intensity of incident light [23]:

$$I_{out} = C_1 I_{in} X^{C_2} \quad (6)$$

Where:  $C_1$  and  $C_2$  depend primarily on the type of light and the bioreactor geometry (dimensionless). The sets of

linear, nonlinear and differential equations used in the above-mentioned models were solved by using MATLAB software version (R2012b).

### 4- Results and Discussion

#### 4.1. Identification of microalgae isolates

The DNA concentrations were measured and found to be 25 and 14, respectively. The extracted DNA molecules were used as templates for amplifying the 16SrRNA genes and ITS genes, using universal primers. The resulted amplification products were visualized as intense, single bands on a 1.5% agarose gel stained with ethidium bromide as shown in Fig. 3.

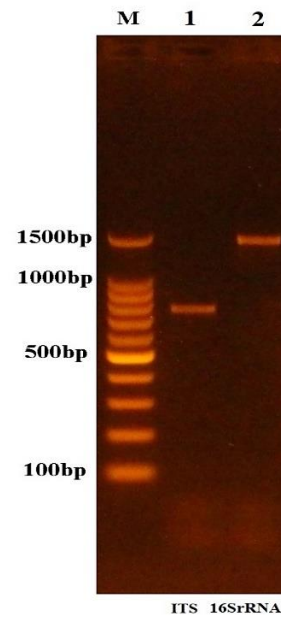


**Fig. 3.** The Amplification of the 16S rRNA and ITS Gene of an Unidentified Microalgae Species Were Seen by Fractionation on a 1.5% Agarose Gel Electrophoresis, which Was Subsequently Stained with Ethidium Bromide

#### 4.2. Microalgae sequencing and growth

In order to classify microalgae, sequencing of the 16S rRNA and ITS genes have been widely used as a crucial tool for identification due to its presence in nearly all types of microalgae [24]. The 16S rRNA gene, with a length of 1500 bp, has remained functionally conserved over time and is large enough to allow for identification of genus and species of isolates [25]. After editing and trimming, the sequences were submitted to NCBI GenBank and compared to other sequences available through the GenBank online BLAST software. The BLAST results showed sequence homology and differences between the sequencing results and other bacterial species submitted to NCBI, as shown in Table 1. The results indicated the existence and characterization of new two different types of green and blue-green algae.

**Table 1.** Identification of the Isolates and GenBank Number of the New Strains of Microalgae used in Cathode Compartment of the PMDC

Isolate No.	Description	Ident %	Accession	New Accession	New strain
1	<i>Coelastrella</i> sp.	99.68%	OM964573.1	ON420725.1	<i>Coelastrella</i> sp. strain AMSZZI1 internal transcribed spacer 1, partial sequence; 5.8S ribosomal RNA gene, complete sequence; and internal transcribed spacer 2, partial sequence
2	<i>Mariniradius saccharolyticus</i>	96.74%	NR_117078.1	ON420764.1	<i>Mariniradius saccharolyticus</i> strain AMSZZI2 16S ribosomal RNA gene, partial sequence

Due to the heavy healthy growth of microalgae in the biocathode chamber, a visible and clear microalgae-based biofilm was observed on the cathode electrode in addition to the suspended microalgae growing profusely in the bulk of the catholyte. Fig. 4 illustrates the SEM images for the microalgae-based biofilm in the cathodic compartment of the PMDC after 90 and 180 days of operation. It is obvious the difference in the texture of the biofilm due to the increased development of the microalgae-based biofilm after 180 days of continuous operation of the PMDC system.

Results from the BLAST software showed sequence homology and differences between sequencing results and other bacterial species submitted to NCBI as shown in Table 1. These results indicated that the 16 S rRNA gene was highly variable among its species, so this gene can be used in future to identify unknown species of this blue-green at the same molecular level, whereby, ITS can be used in the future to identify unknown species of green algae.

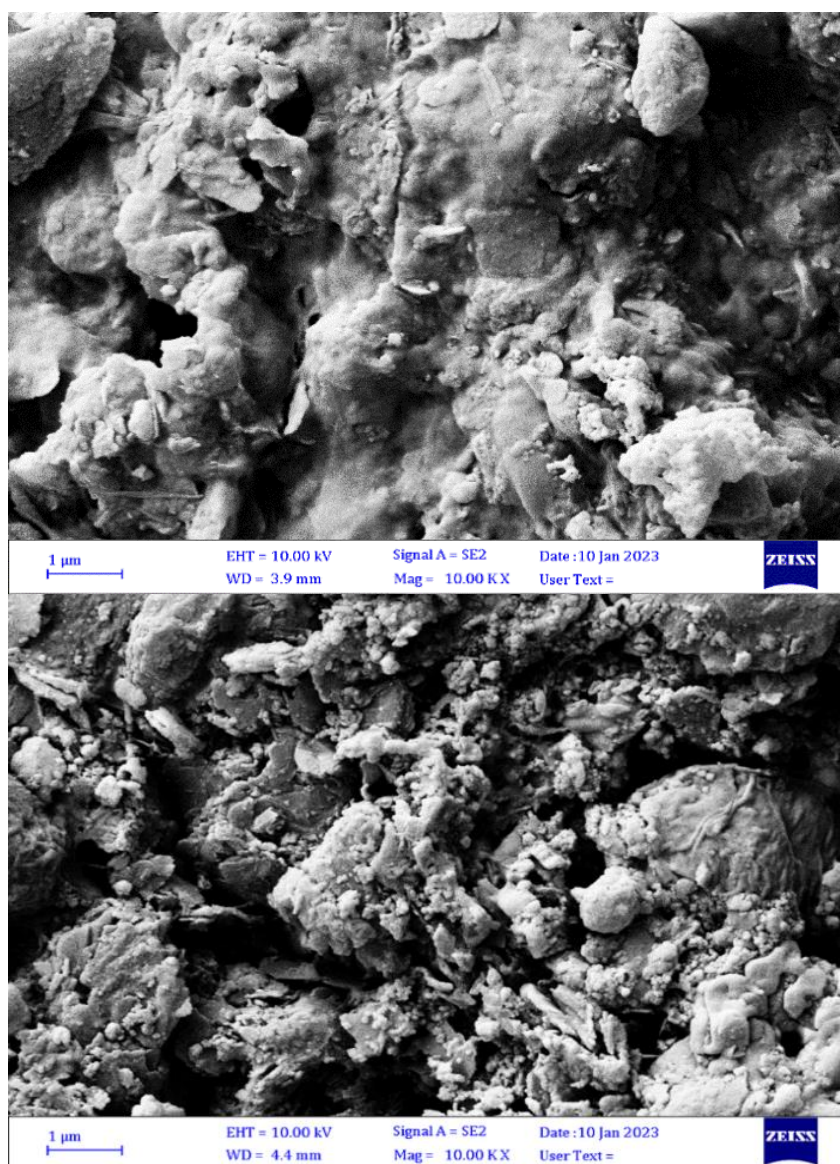


**Fig. 4.** SEM Images of the Microalgae Growth on the Cathode in the TC-PMDC; (Upper Image) after 90 Days Operation, (Lower Image) after 180 Days Operation

#### 4.3. Microalgae growth and DO concentration in the biocathode chamber

In the PMDC system, achieving high growth rates of microalgae is an important step towards integrated bioenergy production. The microalgae growth profile and dissolved oxygen concentration (DO) in the biocathode compartments are shown in Fig. 5 of the PMDC system.

The profiles of microalgae concentration and DO concentration in the biocathode compartment revealed three distinct phases of microalgae growth and DO concentration throughout the entire operation period. During phase 1, which lasted for the initial five days, the concentration of microalgae was relatively low, and the growth rate was slow. However, as the operation progressed, the concentration of DO increase. Subsequently, from day 6 to day 97, the concentration of microalgae steadily increased, indicating a favorable growth environment. Phase 2 of the PMDC operation, occurring after day 97, was marked by a decrease in microalgae concentration over a two-week period, while the DO concentration remained relatively stable. The decline in microalgae concentration could be attributed to various factors, such as growth limitations, competition within the microbial community, or changes in environmental conditions. Growth limitations may have arisen from nutrient depletion, imbalances, changes in light availability, or unfavorable pH levels, which could have negatively impacted microalgae growth. Additionally, competition among microorganisms within the PMDC system might have influenced the microalgae population. However, the stable DO concentration suggests that oxygen production and availability were maintained at a sufficient level during Phase 2. Further

investigation is required to comprehensively understand the factors underlying the observed decrease in microalgae concentration and the stability of DO levels during this phase. Throughout phase 3 which commenced after 110 days of continuous operation, both the microalgae and DO concentrations continued to increase although the microalgae concentration exhibited noticeable fluctuations. The observed variations in the later portion of the microalgae concentration profile may potentially be attributed to causes that extend beyond the inherent life cycle of microalgae. These supplementary elements include, but are not limited to, the availability of carbon dioxide (CO<sub>2</sub>) in the anode compartment, the level of light intensity, and the composition of the growth media. According to the findings of isolates [21], several factors, such as physiological circumstances, possess the capacity to influence the development of microalgae.

Despite these fluctuations, the DO concentration remained relatively sufficient and stable maintaining a level of  $\geq 6.5$  mg/L. This concentration of DO is crucial as it serves as a potential reductant necessary for power production in the PMDC system. The observed fluctuations in microalgae concentration during phase 3 may be attributed to various factors, such as nutrient availability, light intensity, or changes in the microbial community composition. These factors can influence the growth dynamics of microalgae and result in fluctuating concentrations. The consistent and sufficient DO concentration throughout phase 3 is a positive outcome for power production in the PMDC. The availability of an adequate DO concentration supports efficient microbial activity and facilitates the transfer of electrons, ultimately contributing to sustained power generation.

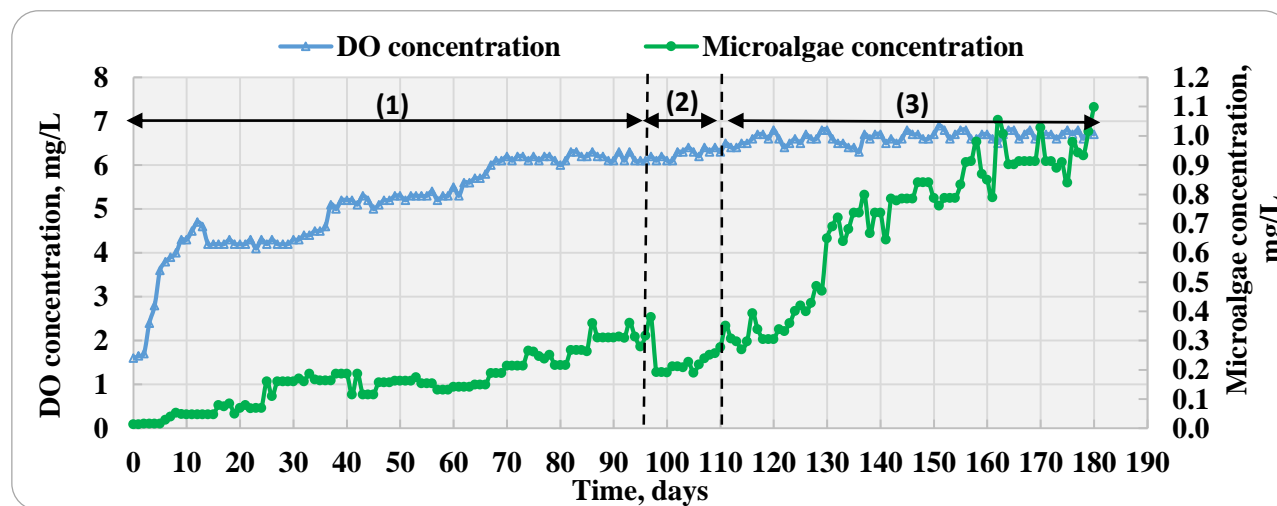


Fig. 5. Profiles of DO and Microalgae Concentrations in the Biocathodic Compartment of PMDC Systems

#### 4.4. Models' predictions

The predicted results for microalgae growth in the biocathodes versus the experimental results are given in Fig. 6. The dynamic model, incorporating dynamic equations, a kinetic expression, and a light transfer model indicated a considerable fitting. The PMDC had a

determination coefficient ( $R^2$ ) value of 0.830, suggesting that the model explained approximately 83% of the observed variance in microalgae growth. These results suggested that the dynamic model provides a robust description of microalgae growth in the different PMDCs designs.

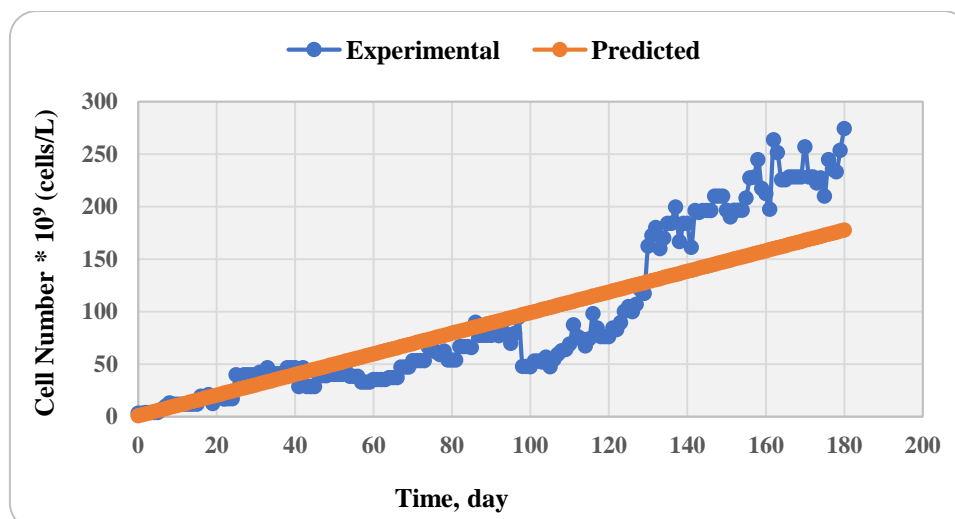


Fig. 6. Predicted and Experimental Results for the Microalgae Growths in the Biocathodes of the PMDC Systems

#### 4.5. Performance of PMDC

Performance of the PMDC after 180 days of continuous operation was significant in regard of organic content removal, power generation, and salinity elimination. One of the most critical factors contributing to the high organic removal efficiency is the creation of favorable anaerobic conditions in the anodic compartment of the PMDC. These anaerobic conditions play an important role in promoting the activity of anaerobic microorganisms, and accordingly facilitating the degradation of organic pollutants. The profile of organic content removal from actual wastewater in the anode compartment of the PMDC is presented in Fig. 7. Despite some fluctuations in the COD removal efficiency, the results showed a noticeable reduction after the first day of operation. Maximum and average removal efficiency of COD was found to be 99.11% and 92.15%, respectively. This promising result could be attributed to the nature of real wastewater contents and composition which was a favorable substrate for the biofilm species. Compared to the previously reported studies, the promising result obtained in this study revealed significant removal efficiency of organic content from wastewater. Kokabian et al. [3] studied the performance of an algae biocathode-PMDC fed with glucose-based synthetic solution in the anodic compartment. The COD removal efficiencies were reported to be in the range of 58%-64%. Das et al. (2020) [26] evaluated the performance of *Oscillatoria* sp. biocathode-PMDC which was fueled with dairy wastewater in the anodic chamber and achieved a COD removal efficiency of 78.45%. Hui et al. [27] proposed 95% COD removal efficiency in a *Chlorella vulgaris*-based biocathode of a cylindrical PMDC for landfill leachate treatment. Bejjanki et al. [28] reported 80.2 ± 0.5% COD elimination efficiency from dairy wastewater in a triple chambered cylindrical PMDC using *Oscillatoria* sp. as the biocathode.

The power generation in the PMDC system was evaluated as a key outcome of this sustainable technique. Profile of the power recovery in the PMDC system is also

given in Fig. 7. The power generation results obtained in the PMDC over the 180-day period exhibited an intriguing pattern characterized by fluctuations and instability. Initially, there was notable increase in the power output during the first 10 days indicating successful microbial colonization and acclimation within the system. This surge in power output could be attributed to enhanced metabolic activity and favorable conditions for electron transfer processes. However, this was followed by a subsequent drop in power generation until day 16, which could be attributed to factors such as microbial community shifts or temporary disruptions in the system's equilibrium. Following day 16, there was a notable recovery phase, with power generation increasing again and reaching a maximum power generation of 420 mW/m<sup>3</sup> and a current density of 1234 mA/m<sup>3</sup>. This energy recovery suggested that the microbial community might have adapted to the changing conditions, resulted in improved power generation. Hence, the results observed in this study were significant compared to the previously reported findings. Bejjanki et al. [28] reported a power density value of 44.1 ± 1.0 mW/m<sup>2</sup> obtained in a PMDC fueled with dairy wastewater and designed with *Oscillatoria* sp. as a biocathode. Zamanpour et al. [29] studied the power generation in two microbial desalination cells (MDCs) of different TDS concentrations. The differences in the power output can be attributed to several factors including, but not limited to the cells geometric design, hydraulic retention time in the cell, type of wastewater and its organic content concentration, TDS concentration and degree of salinity, number and material of electrodes, type of biomass within the anodic biofilm, and microalgae-based biocathode in the PMDC which may contributed to the increased power density. The photosynthetic activity of the microalgae-based biocathode can lead to enhanced electron transfer and metabolic activity resulting in improved power output.

On the other hand, normally the desalination efficiency of a PMDC can be assessed by its ability to remove total dissolved solids (TDS) from saline or brackish aqueous

solution. Results of the desalination efficiency for the PMDC is displayed in Fig. 7. The profile of TDS elimination efficiency demonstrated that during the first 20 days, when the NaCl-based synthetic saline solution

was used, the PMDC achieved a maximum TDS removal efficiency of 21.5% and an average removal efficiency of 16.03%.

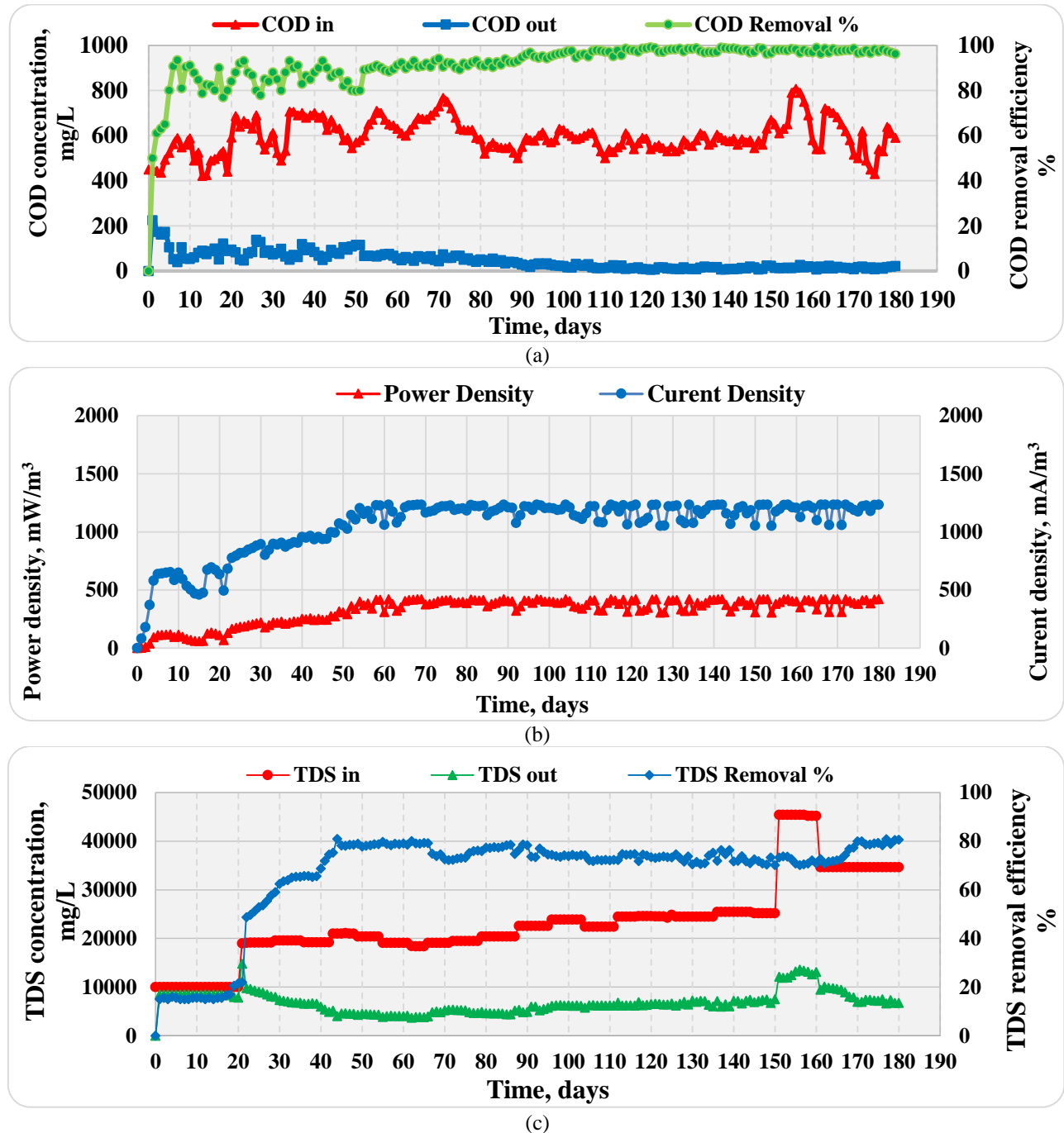


Fig. 7. Profiles of (a) Organic Content Removal (COD), (b) Power Generation, and (c) Salinity Elimination

This observation indicated that the PMDC was able to partially remove TDS from the synthetic saline water. In the subsequent 160 days, the synthetic saline solution in the desalination chamber of the PMDC was replaced with real seawater

Maximum and average removal efficiencies of TDS recorded during the second phase were 81% and 75%, respectively indicating a substantial reduction in the salinity content. The improved TDS removal efficiency

observed during the second phase could be attributed to the fact that the real seawater contains a more complex composition with additional components such as minerals, organic matter, and dissolved solids. These components may contribute to improved conductivity and electrochemical reactions resulted in enhanced TDS removal.

Additionally, the microbial community within the PMDC system might adapted and performed more

efficiently when exposed to real seawater leading to improved TDS removal. In addition to the significant desalination efficiency obtained in this system, no observable fouling of cation exchange membrane (CEM) and anion exchange membrane (AEM) was noticed after 6 months of continuous operation despite the heavy growth of bacterial and microalgae species as well the content of suspended solids in the actual influents fed to the PMDC which may cause membranes fouling and the subsequent deterioration of the PMDC performance.

It is worth noting that the synthetic saline water phase represents a controlled environment since the concentration of salts is consistent. However, the introduction of real seawater to the PMDC system resulted in a significant improvement in the removal efficiency of TDS compared to the synthesis saline water stage. This improvement suggested that the PMDC system is highly recommended for field applications to desalinate real saline waters of various concentrations and compositions. The presence of different salt ions, impurities, and contaminants in real seawater, which are absent or extremely limited in the synthetically prepared saline water, may have played a vital role in enhancing the performance of the PMDC system. The specific properties and mechanisms of the suggested PMDC were likely contributed to its improved removal efficiency in the presence of real saline water. The ability to achieve removal efficiencies exceeding 80% in real saline water is a positive outcome, indicating the potential of the PMDC system for salt removal in real-world scenarios. On the other hand, hydraulic retention time (HRT) may affect the desalination process. According to Morel et al. [30], a longer HRT can lead to back-diffusion of ions due to the concentration gradient between the desalination chamber and adjacent chambers. Therefore, the promising desalination efficiencies observed for the suggested PMDC indicated the proper value of the HRT. The obtained results in this study were significantly higher than the maximum desalination efficiency of 40% observed by Kokabiana and Gude [6] for an algae-biocathode PMDC injected into the desalination chamber using a synthetically prepared NaCl-based saline solution with an initial TDS concentration of 10,000 mg/L. Nadzri et al. [31] investigated the performance of a photosynthetic microbial desalination cell (PhMDC) using *Chlamydomonas* sp. (UKM6) and *Scenedesmus* sp. (UKM9) as biocatalysts. The desalination efficiencies were of 44% and 32% observed in the PhMDC-UKM9 and PhMDC-UKM6, respectively, using a synthetically prepared saline solution of 35000 mg TDS/L. Bejjanki et al. [28] designed a cylindrical three-chamber PMDC using *Oscillatoria* sp. as the biocathode for the treatment of dairy wastewater. The results showed that the maximum desalination efficiency was  $65.8 \pm 0.5\%$ . Barahoei et al. [15] for a three-chamber chemical photosynthesis desalination (CPDC) cell fed with an initial concentration of 12000 mg/L of a synthetic NaCl-based salt solution. The maximum removal efficiency achieved was 69%.

Hence, the differences in TDS removal efficiency in the previous studies could be due to differences in the type of biocatalyst used in the biocathode and/or bio anode, the type of substrate in the anodic section, and the geometric design of the PMDC.

## 5- Conclusion

The study successfully characterized *Coelastrella* sp. and *Mariniradius saccharolyticus*, two distinct species of green and blue-green microalgae, through the analysis of 16S rRNA and ITS genes. The generated sequences, after careful editing and trimming, were deposited in the NCBI GenBank for comparative analysis using the BLAST program available online. Additionally, we monitored the growth of microalgae and dissolved oxygen (DO) concentration in the biocathode chamber, comparing our observations with a microalgae model.

Remarkably, the PMDC system demonstrated exceptional performance in the removal of organic content from actual domestic wastewater. The achieved desalination efficiency reached an impressive 80.95%, and the system exhibited a peak power output of 420 mW/m<sup>3</sup>. These findings suggest the potential of the PMDC system for effective wastewater treatment and energy production.

## Acknowledgment

The authors express their gratitude to the staff of Al-Faw Water Station for their valuable technical assistance and consistent provision of authentic saline seawater samples. The authors acknowledge the Department of Environmental Engineering and the ASCo Learning Center for their generous help in facilitating the laboratory work. The authors are thankful to the dedicated workers at the Al-Rustamia sewage treatment facility for their consistent and invaluable contribution in supplying fresh sewage on a daily basis.

## References

- [1] B. E. Logan, "Microbial fuel cells," John Wiley & Sons, 2008, <https://doi.org/10.1002/9780470258590>
- [2] S. S. Jaroo, G. F. Jumaah, and T. R. Abbas, "Photosynthetic microbial desalination cell to treat oily wastewater using microalgae *Chlorella vulgaris*," *Civil Engineering Journal*, vol. 5, pp. 2686-2699, 2019, <https://doi.org/10.28991/cej-2019-03091441>
- [3] B. Kokabian, V. G. Gude, R. Smith, and J. P. Brooks, "Evaluation of anammox biocathode in microbial desalination and wastewater treatment," *Chemical Engineering Journal*, vol. 342, pp. 410-419, 2018, <https://doi.org/10.1016/j.cej.2018.02.088>
- [4] R. M. Khazaal and Z. Z. Ismail, "Optimization and Modeling the Performance of a Mediator-less Microbial Fuel Cell Using Butler-Volmer-Monod Model," *Journal of Engineering*, vol. 26, no. 9, pp. 83-94, 2020, <https://doi.org/10.31026/j.eng.2020.09.06>

- [5] I. Gajda, J. Greenman, C. Melhuish, and I. Ieropoulos, "Self-sustainable electricity production from algae grown in a microbial fuel cell system," *Biomass and Bioenergy*, vol. 82, pp. 87-93, 2015, <https://doi.org/10.1016/j.biombioe.2015.05.017>
- [6] B. Kokabian and V. G. Gude, "Sustainable photosynthetic biocathode in microbial desalination cells," *Chemical Engineering Journal*, vol. 262, pp. 958-965, 2015, <https://doi.org/10.1016/j.cej.2014.10.048>
- [7] A. S. Commault, G. Lear, P. Novis, and R. J. Weld, "Photosynthetic biocathode enhances the power output of a sediment-type microbial fuel cell," *New Zealand Journal of Botany*, vol. 52, pp. 48-59, 2014, <https://doi.org/10.1080/0028825X.2013.870217>
- [8] C. Wu, X.-W. Liu, W.-W. Li, G.-P. Sheng, G.-L. Zang, Y.-Y. Cheng, N. Shen, Y.-P. Yang, and H.-Q. Yu, "A white-rot fungus is used as a biocathode to improve electricity production of a microbial fuel cell," *Applied Energy*, vol. 98, pp. 594-596, 2012, <https://doi.org/10.1016/j.apenergy.2012.02.058>
- [9] L. Solden, K. Lloyd, and K. Wrighton, "The bright side of microbial dark matter: lessons learned from the uncultivated majority," *Current Opinion in Microbiology*, vol. 31, pp. 217-226, 2016, <https://doi.org/10.1016/j.mib.2016.04.020>
- [10] S. Rasoul-Amini, Y. Ghasemi, M. H. Morowvat, and A. Mohagheghzadeh, "PCR amplification of 18S rRNA, single cell protein production and fatty acid evaluation of some naturally isolated microalgae," *Food Chemistry*, vol. 116, no. 1, pp. 129-136, 2009, <https://doi.org/10.1016/j.foodchem.2009.02.025>
- [11] P. M. Novis, C. Halle, B. Wilson, and L. A. Tremblay, "Identification and characterization of freshwater algae from a pollution gradient using rbcL sequencing and toxicity testing," *Archives of Environmental Contamination and Toxicology*, vol. 57, pp. 504-514, 2009, <https://doi.org/10.1007/s00244-009-9312-0>
- [12] U. John, S. Beszteri, G. Gloeckner, R. Singh, L. Medlin, and A. D. Cembella, "Genomic characterisation of the ichthyotoxic prymnesiophyte *Chrysochromulina polylepis*, and the expression of polyketide synthase genes in synchronized cultures," *European Journal of Phycology*, vol. 45, no. 3, pp. 215-229, 2010, <https://doi.org/10.1080/09670261003746193>
- [13] M. B. Aldin, N. M. Ardalan, and K. A. Jassim, "Isolation and Molecular Characterization of *Acanthamoeba* spp. from Iraqi Patients with Keratitis," *Baghdad Science Journal*, Nov. 2023., <https://doi.org/10.21123/bsj.2023.8059>
- [14] Pandey, S., I. Narayanan, R. Vinayagam, R. Selvaraj, T. Varadavenkatesan, and A. Pugazhendhi, "A Review on the Effect of Blue Green 11 Medium and its Constituents on Microalgal Growth and Lipid Production," *Journal of Environmental Chemical Engineering*, pp. 109984, 2023., <https://doi.org/10.1016/j.jece.2023.109984>
- [15] M. Barahoei, M. S. Hatamipour, M. Khosravi, S. Afsharzadeh, and S. E. Feghipour, "Salinity reduction of brackish water using a chemical photosynthesis desalination cell," *Science of the Total Environment*, vol. 779, p. 146473, 2021, <https://doi.org/10.1016/j.scitotenv.2021.146473>
- [16] S. A. Jassim and N. J. Kandala, "Molecular Detection of Enterotoxin Genes of Multiresistant *Staphylococcus aureus* Isolates from Different Sources of Food," *Iraqi Journal of Science*, vol. 62, no. 1, pp. 61-74, 2021, <https://doi.org/10.24996/ij.s.2021.62.1.6>
- [17] H. K. Abbas and A. M. Ghareeb, "Prevalence of some Virulence Genes in *Staphylococcus aureus* Isolated from Iraqi Infertile Male Patients and its Effects on Sperm Parameters," *Iraqi Journal of Biotechnology*, vol. 22, no. 1, pp. 163-172, 2023.
- [18] T. Cheng, C. Xu, L. Lei, C. Li, Y. Zhang, and S. Zhou, "Barcoding the kingdom Plantae: new PCR primers for ITS regions of plants with improved universality and specificity," *Molecular Ecology Resources*, vol. 16, pp. 138-149, 2016, <https://doi.org/10.1111/1755-0998.12438>
- [19] L. N. Ponpandian, S. O. Rim, G. Shanmugam, J. Jeon, Y.-H. Park, S.-K. Lee, and H. Bae, "Phylogenetic characterization of bacterial endophytes from four *Pinus* species and their nematocidal activity against the pine wood nematode," *Scientific Reports*, vol. 9, p. 12457, 2019, <https://doi.org/10.1038/s41598-019-48745-6>
- [20] S. Garcha, N. Verma, and S. K. Brar, "Isolation, characterization and identification of microorganisms from unorganized dairy sector wastewater and sludge samples and evaluation of their biodegradability," *Water Resources and Industry*, vol. 16, pp. 19-28, 2016, <https://doi.org/10.1016/j.wri.2016.10.002>
- [21] T. G. Albadri and M. A. Alaubdy, "Molecular Identification of *Roseomonas mucosa* and Determination of Some of Its Virulence Factors," *Iraqi Journal of Agricultural Sciences*, vol. 54, no. 2, pp. 581-588, 2023, <https://doi.org/10.36103/ij.as.v54i2.1734>
- [22] A. M. Sadeq and Z. Z. Ismail, "Sustainable Application of Tubular Photosynthesis Microbial Desalination Cell for Simultaneous Desalination of Seawater for Potable Water Supply Associated with Sewage Treatment and Energy Recovery," *Science of the Total Environment*, vol. 875, p. 162630, 2023, <https://doi.org/10.1016/j.scitotenv.2023.162630>
- [23] R. Filali, S. Tebbani, D. Dumur, S. Diop, A. Isambert, D. Pareau, and F. Lopes, "Estimation of *Chlorella vulgaris* growth rate in a continuous photobioreactor," *IFAC Proceedings Volumes*, vol. 44, pp. 6230-6235, 2011, <https://doi.org/10.3182/20110828-6-IT-1002.02025>
- [24] I. Suikaitė, G. Vanseviciūtė, and J. Koreivienė, "An overview of the distribution and ecology of the alien cyanobacteria species in Europe," *Oceanological and Hydrobiological Studies*, vol. 52, no. 3, pp. 312-332, 2023, <https://doi.org/10.26881/oahs-2023.3.06>

- [25] M. B. Qader and M. H. AlKhafaji, "Detection of Bacterial Contamination of Imported Chicken Meat in Iraq," *Iraqi Journal of Science*, vol. 60, pp. 1957-1966, 2019.
- [26] I. Das, M. M. Ghangrekar, R. Satyakam, P. Srivastava, S. Khan, and H. N. Pandey, "On-site sanitary wastewater treatment system using 720-L stacked microbial fuel cell: case study," *Journal of Hazardous, Toxic, and Radioactive Waste*, vol. 24, no. 3, p. 04020025, 2020, [https://doi.org/10.1061/\(ASCE\)HZ.2153-5515.0000518](https://doi.org/10.1061/(ASCE)HZ.2153-5515.0000518)
- [27] W. J. Hui, E. M. David, and J. Huang, "Using *C. vulgaris* assisted microbial desalination cell as a green technology in landfill leachate pre-treatment: a factor-performance relation study," *Journal of Water Reuse and Desalination*, vol. 10, no. 1, pp. 1-16, 2020, <https://doi.org/10.2166/wrd.2019.073>
- [28] D. Bejjanki, K. Muthukumar, T. K. Radhakrishnan, A. Alagarsamy, A. Pugazhendhi, and S. N. Mohamed, "Simultaneous bioelectricity generation and water desalination using *Oscillatoria* sp. as biocatalyst in photosynthetic microbial desalination cell," *Science of The Total Environment*, vol. 754, p. 142215, 2021, <https://doi.org/10.1016/j.scitotenv.2020.142215>
- [29] M. K. Zamanpour, H. R. Kariminia, and M. Vosoughi, "Electricity generation, desalination and microalgae cultivation in a biocathode-microbial desalination cell," *Journal of Environmental Chemical Engineering*, vol. 5, no. 1, pp. 843-848, 2017, <https://doi.org/10.1016/j.jece.2016.12.045>
- [30] A. Morel, K. Zuo, X. Xia, J. Wei, X. Luo, P. Liang, and X. Huang, "Microbial desalination cells packed with ion-exchange resin to enhance water desalination rate," *Bioresource Technology*, vol. 118, pp. 43-48, 2012, <https://doi.org/10.1016/j.biortech.2012.04.093>
- [31] N. A. A. Nadzri, N. H. M. Yasin, M. H. A. Bakar, S. Thanakodi, M. N. I. Salehmin, M. S. Takriff, M. F. N. Aznan, and T. Maeda, "Photosynthetic microbial desalination cell (PhMDC) using *Chlamydomonas* sp. (UKM6) and *Scenedesmus* sp. (UKM9) as biocatalysts for electricity production and water treatment," *International Journal of Hydrogen Energy*, vol. 48, no. 31, pp. 11860-11873, 2023, <https://doi.org/10.1016/j.ijhydene.2023.01.142>

## نمو الطحالب الدقيقة في حجرة الكاثود الاحيائي لخلية التحلية الاحيائية بالتركيب الضوئي: التشخيص الجزيئي، دراسة النمذجة، وتقييم الاداء

أحمد مصطفى صادق<sup>١</sup>، زينب زياد اسماعيل<sup>١\*</sup>

<sup>١</sup> قسم الهندسة البيئية، كلية الهندسة، جامعة بغداد، بغداد، العراق

### الخلاصة

هذه الدراسة تهدف إلى توصيف وتحديد شامل للطحالب الدقيقة التي تعيش في حجرة الكاثود الاحيائي في خلية التحلية الاحيائية الضوئية (PMDC) كما تضمنت الدراسة أيضًا نمذجة نمو الطحالب الدقيقة في الكاثود الحيوي واستكشاف العلاقة بين نمو الطحالب الدقيقة وتكوين الأكسجين المذاب (DO) داخل الكاثود الاحيائي. بالإضافة إلى ذلك، تم تقييم الأداء العام لللية التحلية الاحيائية الضوئية استنادًا إلى ثلاث جوانب رئيسية: (١) إزالة المواد العضوية من مياه الصرف الصحي المنزلي الحقيقية المغذاة إلى حجرة الأنود، (٢) إزالة الملوحة من مياه البحر الحقيقية في حجرة التحلية، (٣) توليد الطاقة في خلية التحلية الاحيائية الضوئية. أظهرت النتائج وجود نوعين مميزين من الطحالب الدقيقة داخل حجرة الكاثود الاحيائي وتحديدًا *Coelastrella sp.* و *Mariniradius saccharolyticus* حيث تم تحديد هذه الأنواع بشكل شامل باستخدام تسلسل الجينات 16S rRNA و ITS داخل حجرة الكاثود. بعد تحرير وتعديل التسلسلات، تم تقديم البيانات الناتجة بعناية إلى قاعدة البيانات العالمية (NCBI GenBank) ومقارنتها مع تسلسلات أخرى باستخدام برنامج BLAST. والاهم بشكل عام، أظهرت النتائج المختبرية مع نتائج النمذجة ترابطًا جيدًا مع معامل تحديد ( $R^2$ ) ٠,٨٣، وفقًا للنمذجة المستخدمة كذلك تم الحصول على إزالة كاملة للمحتوى العضوي من مياه الصرف الصحي الحقيقية بمقدار ٩٩,١١% وكذلك اعلى كفاءة في إزالة الملوحة بنسبة ٨٠,٩٥% متزامنة مع توليد طاقة كهربائية بمقدار بلغ ٤٢٠ ميلي واط/متر مكعب في الخلية.

الكلمات الدالة: التوصيف الميكروبي، الطحالب الدقيقة، بنك الجينات NCBI، نمذجة حركية النمو، الكاثود الحيوي، خلية الوقود الحيوي.